

Invasive alga reaches California

The alga has been identified that threatens to smother Californian coastal ecosystems.

The recent discovery of the marine green alga *Caulerpa taxifolia* on the Californian coast^{1,2} has raised public concern about the potential danger of a new invasion similar to the one endured by the Mediterranean Sea over the past decade. A small colony of *C. taxifolia* introduced into the Mediterranean in 1984^{3,4} from a public aquarium⁵ has spread to more than 6,000 hectares today, outcompeting native species and seriously reducing diversity in areas of the northwestern Mediterranean⁶. This invasive strain of *C. taxifolia* differs from tropical populations in that it is much larger, grows more vigorously, does not rely on sexual reproduction, and is resistant to low temperatures^{4,6,7}. Here we evaluate the risk of invasion by Californian *C. taxifolia* by comparing it genetically with the Mediterranean and aquarium strain, as well as with native tropical populations. Our results show that the Californian alga is the same as the invasive Mediterranean strain, calling for its rapid eradication to prevent a new invasion.

Colonies of *C. taxifolia*, morphologically similar to the Mediterranean strain, have been reported from Carlsbad and Huntington Harbour, California. *C. taxifolia* covers 3,500 square metres at Carlsbad and is dispersed over 20,000 square metres at Huntington Harbour. We extracted DNA from algal samples collected in these areas in independent analyses in two laboratories (Geneva, Switzerland, and Fresno, California). The internal transcribed spacer of ribosomal DNA (ITS rDNA) was amplified by using the polymerase chain reaction and then cloned⁵, and the sequence data were used to examine intraspecific variability within *C. taxifolia*. Five clones were sequenced for each isolate in Geneva; two specimens analysed in Fresno were sequenced directly. We compared Californian alga sequences with 148 ITS rDNA sequences obtained from 32 *C. taxifolia* specimens collected from all over the world.

Eleven out of twelve Californian sequences were found to be identical to all aquarium and most Mediterranean sequences (Fig. 1a). The single divergent sequence (Carl4), which differs by two nucleotide substitutions, branches with other Mediterranean sequences. This group is clearly separated from all sequences obtained from other isolates of *C. taxifolia*, including tropical strains of this species collected in the Red Sea, Caribbean Sea and the Indo-Pacific (Fig. 1b). Phylogenetic analysis of all *C. taxifolia* ITS rDNA sequences reveals a relatively robust clade (80% bootstrap value) grouping Californian, Mediterranean, aquarium and some

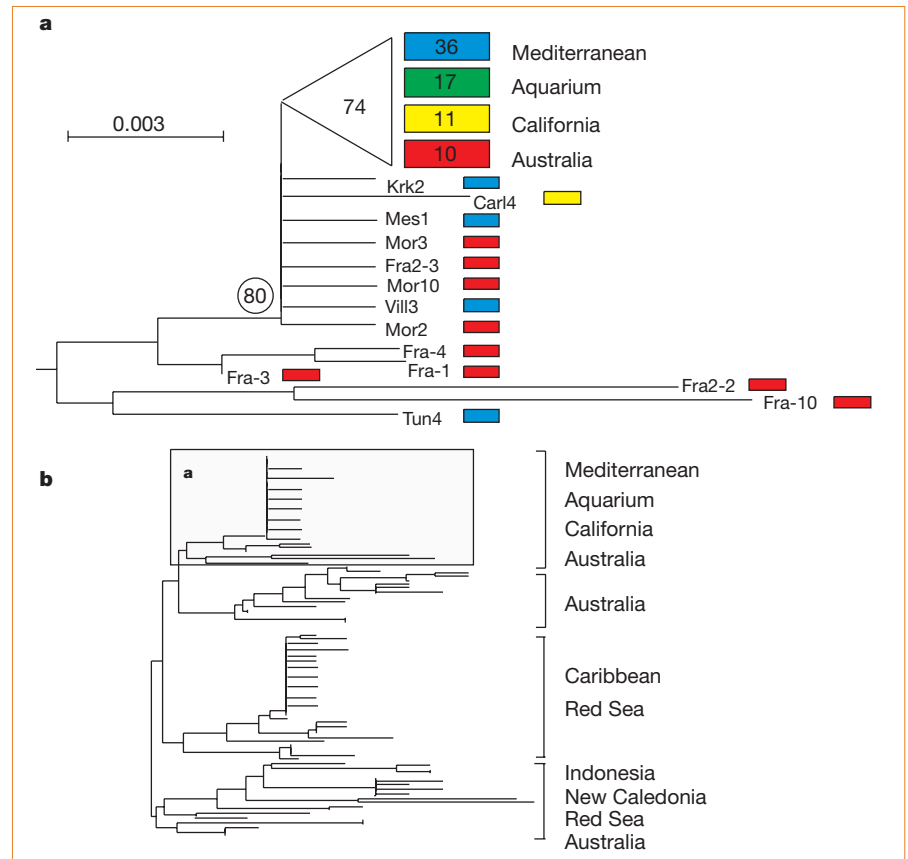


Figure 1 Phylogenetic tree of *C. taxifolia* inferred from 160 complete ITS (internal transcribed spacer) ribosomal DNA sequences by using the neighbour-joining method applied to pairwise sequence distances calculated by the Kimura two-parameter method. **a**, The clade containing all Californian sequences; the origin of different sequences is indicated by coloured rectangles containing the number of identical sequences; number 80 at the base of the clade corresponds to the bootstrap value based on 1,000 replicates. Abbreviations are: Krk (Krk Island, Croatia), Carl (Carlsbad, California), Mes (Messina, Italy), Mor (Moreton Bay, Australia), Fra (Fraser Island, Australia), Vill (Villefranche, France), Tun (Sousse, Tunisia). **b**, Total tree, presenting relationships between algae of different geographical origins. Sampling localities (number of analysed sequences in parentheses) in the Mediterranean Sea: Majorca (3), Saint-Cyprien (3), Le Brusca (3), Toulon (3), Port-Cros (3), Le Lavandou (3), Villefranche (5), Messina (3), Elba (3), Krk (3) and Hvar (3) Islands, Croatia; Sousse, Tunisia (5); aquarium samples: Nancy (3), Stuttgart (5), Geneva (3), Oahu (3), Enoshima (3); sampling localities off the Californian coast: Carlsbad (6) and Huntington Harbour (6); from Australian waters: Townsville⁵ (1), Fraser Island (13), Moreton Bay (18), Port Hacking (5), Lake Conjola (9); in the Caribbean: Puerto-Rico (5), Martinique (7), Guadeloupe (3); from the Red Sea: Safaga, Egypt (21); from Indonesian waters: Djakarta⁹ (1); and from New Caledonia: Noumea (8). Ethanol-fixed specimens of Californian *C. taxifolia* have been deposited in the herbarium of the Botanical Garden in Geneva and in the Jepson Herbarium at the University of California, Berkeley. EMBL accession numbers for the sequences analysed are AJ228960–AJ228999 and AJ299742–AJ299811.

Australian sequences. Thus, the Californian alga belongs to the aquarium–Mediterranean strain.

A particular feature of all aquarium, Mediterranean and Californian (AMC) specimens we examined is the low degree of intra-individual polymorphism of their rRNA genes: 64 sequences from AMC isolates were identical, whereas five were slightly divergent (from 0.4 to 1.1%). Such homogeneity contrasts with the high polymorphism of ITS copies in non-AMC isolates, characterized by intra-isolate sequence divergence ranging from 0.8 to 3.6%.

It is notable that the eastern Australian polymorphic isolates possess ITS copies that are identical to the AMC type (10 out of 46 Australian sequences). This may point to Australia as being the possible native land of the invasive alga, but this needs to be confirmed by analysis of other genetic markers to ascertain the similarity of the strains.

O. Jousson*, **J. Pawlowski***, **L. Zaninetti***, **F. W. Zechman†**, **F. Dini‡**, **G. Di Guiseppe‡**, **R. Woodfield§**, **A. Millar||**, **A. Meinesz¶**

* Université de Genève, Département de Zoologie et Biologie Animale, 1224 Chêne-Bougeries, Switzerland
 e-mail: jousson2@sc2a.unige.ch

†Department of Biology, California State University, Fresno, California 93740, USA
 ‡Università di Pisa, Dipartimento di Etologia, Ecologia ed Evoluzione, 56126 Pisa, Italy
 §Merkel and Associates, San Diego, California 92123, USA
 ||Royal Botanic Gardens, Sydney, New South Wales 2000, Australia
 ¶Université de Nice-Sophia Antipolis, Laboratoire Environnement Marin Littoral, 06108 Nice, France

Imaging

Phase radiography with neutrons

The interaction of neutrons with matter enables neutron radiography¹ to complement X-ray radiography in analysing materials. Here we describe a simple quantitative method that provides a new contrast mechanism for neutron radiography and allows samples to be imaged at low radiation doses. Large phase shifts can be measured accurately from detailed structures not amenable to conventional techniques.

The complexity of interferometry has limited studies on neutron phase imaging. Our non-interferometric phase-measurement technique is appropriate for non-uniform radiation and returns a unique, non-wrapped, smooth, continuous quantitative phase map; it implements a theoretical study² and has been used for other types of radiation, including visible light³, electrons⁴, soft⁵ and hard⁶ X-rays.

We base our analysis on the paraxial transport of intensity equation^{7,8}

$$\frac{2\pi}{\lambda} \frac{\partial I(\mathbf{r}_\perp)}{\partial z} = -\nabla_\perp \times [I(\mathbf{r}_\perp) \nabla_\perp \phi(\mathbf{r}_\perp)] \quad (1)$$

where the wave is described by $\sqrt{I(\mathbf{r}_\perp)} \exp(i\phi(\mathbf{r}_\perp))$, with intensity $I(\mathbf{r}_\perp)$ and phase $\phi(\mathbf{r}_\perp)$; ∇_\perp and \mathbf{r}_\perp are respectively the gradient operator and position vector in the plane perpendicular to the longitudinal optic axis z , λ is the wavelength, and $\partial I(\mathbf{r}_\perp)/\partial z$ is the longitudinal intensity derivative.

We used the beam port of the Neutron Interferometry facility at NIST, operating at a selectable monochromatic wavelength of 4.43 Å. The divergence of the neutron beam was limited by a mask to around 6 milliradians and neutrons illuminated a sample at about 1.8 m from the beam-guide exit. The two-dimensional detector⁹ was 30% efficient and combined an in-beam ⁶Li-ZnS scintillator, light intensifier and mirror. The mirror reflected the light out of the neutron beam and into an optical charge-coupled device camera. Electronic centroiding of images optimized the spatial resolution to 60 μm.

The intensity over a surface is consistent

1. Kaiser, J. *Science* **289**, 222–223 (2000).
2. Dalton, R. *Nature* **406**, 447 (2000).
3. Meinesz, A. & Boudouresque, C. F. *C. R. Acad. Sci. Paris Life Sci.* **319**, 603–613 (1996).
4. Meinesz, A. & Hesse, B. *Oceanol. Acta* **14**, 415–426 (1991).
5. Jousson, O., Pawlowski, J., Zaninetti, L., Meinesz, A. & Boudouresque, C. F. *Mar. Ecol. Prog. Ser.* **172**, 275–280 (1998).
6. Meinesz, A. *et al. Bot. Mar.* **38**, 499–508 (1995).
7. Komatsu, T., Meinesz, A. & Buckles, D. *Mar. Ecol. Prog. Ser.* **146**, 145–153 (1997).
8. Olsen, J. L., Valero, M., Meusnier, I., Boele-Bos, S. & Stam, W. T. *J. Phycol.* **34**, 850–856 (1998).
9. Pighini, M. & Dini, F. *4th International Workshop on Caulerpa taxifolia* (Lerici, Italy, 1999).

with any phase distribution. Equation (1) indicates, however, that the phase does influence the propagation of the intensity. It is therefore possible to visualize phase in a certain plane by allowing a wave to evolve

away from that plane¹⁰ — an example of this is the familiar heat shimmer over a hot road. This effect was used to visualize the neutron phase shift for a North American yellow-jacket wasp (genus *Vespula*) (Fig. 1). A conventional neutron radiograph (Fig. 1a) is compared with a phase-contrast image obtained 1.8 m downstream from the sample using neutrons emanating from a 0.4-mm-diameter pinhole placed at the exit of the beam guide (Fig. 1b). The pinhole sets the limit to the spatial resolution. The improved sensitivity of the image arises from shifts in the neutron phase introduced by the sample.

To retrieve phase quantitatively using equation (1), we require the intensity $I(\mathbf{r}_\perp)$ and intensity derivative $\partial I(\mathbf{r}_\perp)/\partial z$ in the plane of interest. To obtain this, images were

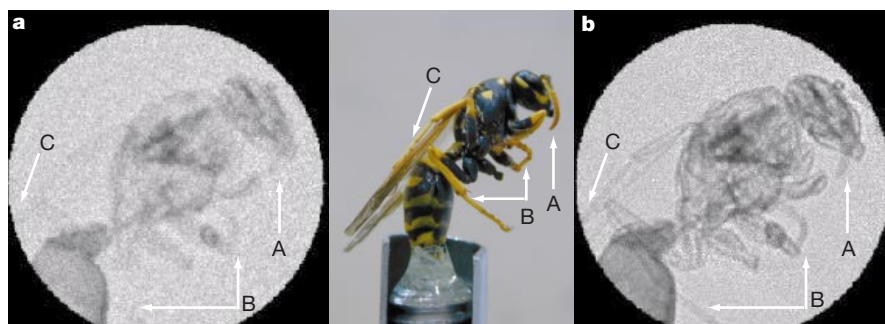


Figure 1 Neutron phase-contrast imaging of a yellow-jacket wasp. **a**, Conventional neutron radiograph. **b**, Phase-contrast image showing greater clarity of finer features such as the antenna (A), legs (B) and projection through the leg and wing (C).

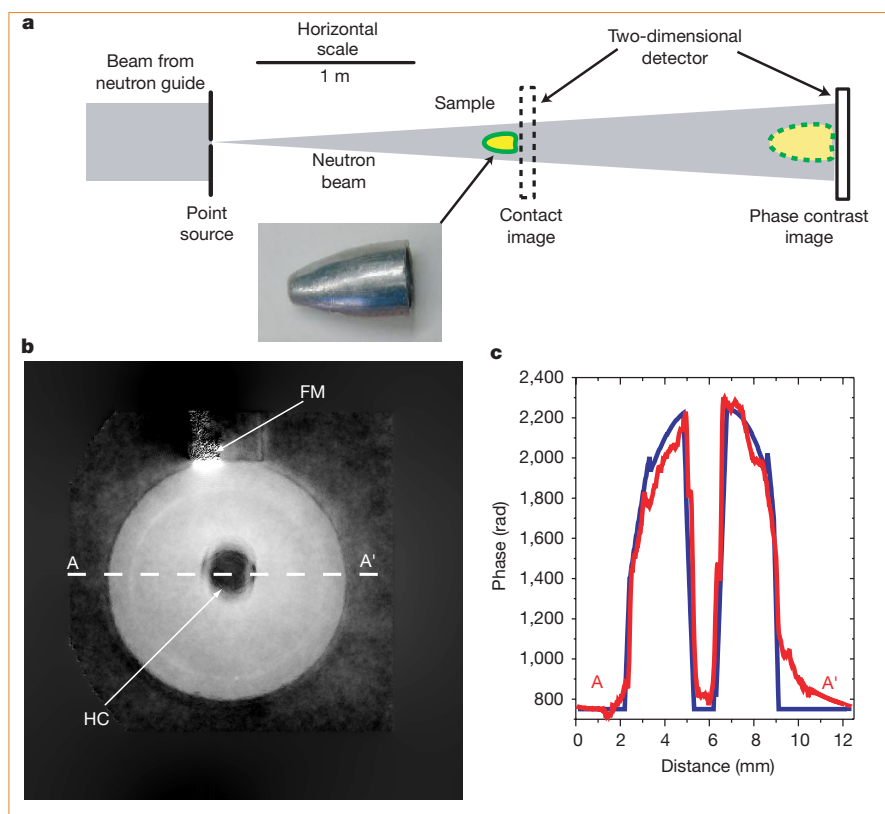


Figure 2 Quantitative neutron phase imaging. **a**, Experimental scheme, with the lead sinker sample shown in the inset. **b**, Quantitative phase map of the Pb sinker showing the hollow core (HC) and fiducial mark artefact (FM). **c**, Quantitative phase profile AA' through the sinker (red) and calculated profile (blue) based on the known shape, scattering length and orientation of the sinker.